J Integr Sci Technol, 2015, 3(2), 28-33 Article

Journal of Integrated
SCIENCE & TECHNOLOGY

Optical absorption and fluorescence spectral analysis of Ho^{3+} ions doped zinc bismuth borate glasses

Manju Lather,[1] Praveen Aghamkar,[1] Sujata Sanghi[2]

[1]*Department of Physics,Chaudhary Devi Lal University, Sirsa-125055, Haryana, India.* [2]*Department of Applied Physics, Guru Jambheshwar University of Science & Technology, Hisar- 125001, Haryana, India*

ABSTRACT

Zinc Bismuth Borate glasses doped with Holmium was prepared by normal melt quenching technique. Optical absorption and photoluminescence spectra of these glasses have been recorded at room temperature. The observed spectra have been analysed on the basis of Judd-Ofelt theory. From this theory various radiative properties such as radiative transition probability, branching ratio, radiative life time and stimulated emission cross-section for the prominent emission levels $^5F_3 \rightarrow {}^5I_8$, $^5F_4 \rightarrow {}^5I_8$, $^5S_2 \rightarrow {}^5I_8$ and $^5F_5 \rightarrow {}^5I_8$ have been evaluated.

Keywords: Judd–Ofelt parameters, Radiative life-time, branching ratio, stimulated emission cross section, Ho^{3+} doped glasses.

INTRODUCTION

Spectroscopy of the lanthanides or rare-earth ions (RE^{3+}) built-in in different dielectrics (crystalline or amorphous glass host matrices) has been one of the most attractive areas of solid-state research since the first demonstration of lasing action in Nd-doped glass by Snitzer in 1961.[1] The applications of RE^{3+} ions are now extended to nearly all important fields of technology. Photoluminescence of Ho^{3+}, Nd^{3+}, Dy^{3+} and Sm^{3+} ions are investigated for application in high-energy particle detector, biomedical lasers, optical data storage, bar-code reading, laser printing, underwater and satellite communication, environment friendly solid- state lighting, etc[2-4]. Even though the 4f electrons of RE^{3+} ions are shielded by the 5s and 5p electrons, the spin–orbit interactions (depending on the number of 4f electrons) exert much influence on the positions of their electronic energy levels. The characteristic emission properties of different RE^{3+} ions ultimately take place due to electronic transitions among these energy levels. The surrounding ligand-field or the host matrix incorporating the RE^{3+} ions also exerts a significant influence on the lasing properties[5].

Address:
Manju Lather
Department of Physics, Chaudhary Devi Lal University,
Sirsa -125055, Haryana, India
Tel: +91-8901046824
Email: lathermanju@yahoo.com

Cite as: *J. Integr. Sci. Technol., 2015, 3(2), 28-33.*

 JIST ISSN 2321-4635

http://pubs.iscience.in/jist

In current years large emphasis has been given to the discovery of new HMO glass compositions for exploitation as RE-doped luminescent hosts. Glasses having bismuth oxide have attained great attention, since they are used in the wide area of applications. The obtained glasses are characterized by high density, high refractive index, extended transmission in mid-IR, high dielectric constant, etc. Hence there has been a growing interest in the synthesis and investigation of microstructure and physical properties of heavy metal oxide (HMO) glasses containing bismuth oxide as a major component. Bismuth oxide (Bi_2O_3) based glasses for their high polarizability have attracted much attention of glass researchers because of their nonlinear optical properties being important for the development of optical information processing technology [6-8]. Bismuth oxide cannot be considered as a glass network former due to low field strength (0.53) of Bi^{3+} ion. However, in combination with B_2O_3 glass former it is possible to obtain glasses in a relatively large compositional ranges. A survey of literature shows that there are many reports available on ternary bismuth borate glasses[9-10]. The properties of the glasses are closely related to inter-atomic forces and potentials in lattice structure. Thus any change in the lattice due to doping can be directly being noticed. Ho^{3+} ion, yet another interesting ion which exhibits eye-safe potential laser emission even at room temperature with a low threshold action has been chosen for doping in zinc bismuth borate glass network.

The aim of this investigation is the study of optical absorption and fluorescence spectra of Ho^{3+} doped ZnO–Bi_2O_3–B_2O_3 glasses and to apply the Judd–Ofelt theory for f–f transitions of Ho^{3+} ion and to evaluate various radiative properties like transition probability, radiative life times of various excited states and emission cross-sections of various emission levels.

JUDD-OFELT THEORY

The absorption spectra of rare earth ions serve as a basis for understanding their radiative properties. The sharp absorption lines arising from the 4f–4f electronic transitions can be electric dipole, magnetic dipole or electric quadrupole in character. The quantitative calculation of the intensities of these transitions has been developed independently by Judd and Ofelt. A brief outline of the Judd–Ofelt theory is given below:

For a rare earth ion, the electric dipole transitions between two states within the 4f configuration are parity forbidden, while the magnetic dipole and electric quadrupole transitions are allowed. For an ion in a medium, the electric dipole transitions become allowed due to the admixture of states from configuration of opposite parity (for example $4f^{N-1}$ 5d) into the 4f configuration. The transition probability depends on the extent of admixture. The intensity of an absorption band is expressed in terms of a quantity called the "oscillator strength". Experimentally, it is given by the area under the absorption band and can be expressed in terms of the absorption coefficient, $\alpha(\lambda)$ at a particular wavelength λ and is given by[11]:

$$f_{expt} = \frac{mc^2}{\pi e^2 N}\int \frac{\alpha(\lambda)}{\lambda^2} d\lambda \quad (1)$$

where $\alpha(\lambda)$= (2.303)OD(λ)/d, OD(λ) is the optical density, d is the thickness of the sample, m and e are the mass and charge of electron, respectively, c is the velocity of light and N is the number of rare earth ions per unit volume.

According to the Judd–Ofelt theory[12], the oscillator strength of a transition between an initial J manifold (S, L, J) and a final J' Manifold (S', L', J') is given by:

$$f_{cal}(aJ,bJ') = \frac{8\pi^2 m\nu}{3h(2J+1)}\left[\frac{\left(n^2+2\right)^2}{9n} S_{ed} + nS_{md}\right] \quad (2)$$

Where

$$S_{ed}[(S,L)J,(S',L')J'] = \sum_{\lambda=2,4,6} \Omega_\lambda \left|\left\langle (S,L)J \left\| U^{(\lambda)} \right\| (S',L')J' \right\rangle\right|^2$$

And

$$S_{md}[(S,L)J,(S',L')J'] = \sum_{\lambda=2,4,6} \Omega_\lambda \left|\left\langle (S,L)J \left\| L+2S \right\| (S',L')J' \right\rangle\right|^2$$

S_{ed} and S_{md} represent the line strengths for the induced electric dipole transitions and the magnetic dipole transitions, respectively.

The three intensity parameters, Ω_λ (λ = 2, 4, 6) are characteristic of a given rare earth ion (in a given matrix) and are related to the radial functions of the state's $4f^N$, the admixing states $4f^{N-1}5d$ or $4f^{N-1}5g$ and the ligand field parameters that characterize the environmental field. These are given by the expression:

$$\Omega_\lambda = (2\lambda+1)\sum_{s,p}\left|A_{s,p}\right|^2 \Xi^2(s,\lambda)(2S+1)^2,\ \lambda = 2,4,6 \quad (3)$$

Where, $A_{s,p}$ are the crystal field parameters of rank s and are related to the structure around the rare earth ion. $\Xi(s,\lambda)$ is related to the matrix elements between the radial wave functions of 4f and admixing levels, e.g., 5d, 5g and the energy difference between two levels. $\left|\left\langle \left\| U^{(\lambda)} \right\| \right\rangle\right|^2$ represents the square matrix elements of the unit tensor operators $U^{(\lambda)}$ connecting the initial and final states.

The matrix elements are calculated in the intermediate coupling approximation[13]. Due to the electrostatic shielding of the 4f electrons by the closed 5p shell electrons, the matrix elements of the unit tensor operator between two energy manifolds in a given rare earth ion do not vary significantly when it is incorporated in different hosts. Therefore, the matrix elements computed for the free ion may be used for calculation in different media and are reported by Weber et al.[14] and Carnall et al.[15]. The reduced matrix elements $\left\langle \left\| L+2S \right\| \right\rangle$ for magnetic dipole transitions are reported by Neilson et al.[16]. The values of Ω_λ obtained from the absorption measurements are used to calculate the radiative transition probability, radiative lifetime of the excited states, branching ratio (which predict the fluorescence intensity of the lasing transition) and stimulated emission cross-section. The radiative transition probability $A_{rad}(aJ,bJ')$ for emission from an initial state aJ to a final bJ' is given by[17]:

$$A_{rad}(aJ,bJ') = \frac{64\pi^4\nu^3 e^2}{3hc^3(2J+1)}\left[\frac{n\left(n^2+2\right)^2}{9} S_{ed} + n^3 S_{md}\right] \quad (4)$$

In case of electric dipole emission, this equation becomes:

$$A_{rad}(aJ,bJ') = \frac{64\pi^4\nu^3 e^2}{3hc^3(2J+1)}\frac{n\left(n^2+2\right)^2}{9} \times \sum_{\lambda=2,4,6}\Omega_\lambda \left|\left\langle (S,L)J \left\| U(\lambda) \right\| (S',L')J' \right\rangle\right|^2 \quad (5)$$

The total radiative emission probability, A_T (aJ) of the excited state SLJ is given by the sum of the A_{rad} (aJ,bJ`) terms calculated over all terminal states b

$$A_T(aJ) = \sum_{bJ'} A_{rad}(aJ,bJ') \quad (6)$$

The fluorescence branching ratio β_r is given as:

$$\beta_r = \frac{A_{rad}(aJ,bJ')}{A_T(aJ)} \quad (7)$$

The radiative lifetimes of the emission state is:

$$\tau_r = \frac{1}{A_T(aJ)} \quad (8)$$

Finally, the stimulated emission cross-section of the fluorescent level is given by:

$$\sigma = \frac{\lambda_p^4 A_{rad}(aJ,bJ')}{8\pi c n^2 \Delta\lambda} \quad (9)$$

where λp is the wavelength of the fluorescence peak and Δλ is the line width obtained by dividing the area of the emission band by its average height. The large value of stimulated emission cross-section and high branching ratio determine the suitability of the materials for good optical devices.

EXPERIMENTAL DETAILS

Glasses having compositions $20ZnO\text{-}xBi_2O_3\text{-}(79{\cdot}5\text{-}x)B_2O_3$ ($15 \le x \le 35$, mol %) doped with 0.5 mol% of Ho^{3+} ions were prepared by melt quench technique. Appropriate amount of chemicals (ZnO, Bi_2O_3, B_2O_3 and Ho_2O_3) having purity above 99.99% were weighed on 0.001% accuracy and mixed thoroughly. The raw mixed materials were melted in a muffle furnace in air (at 1373K for 0.5h). The crucible was shaken frequently after every 10 minutes for the homogeneous mixing of all the constituents. The melt was quenched at room temperature by pouring between two stainless steel plates. The samples were polished for spectral and other investigations.

The density (D) of all the glasses was measured by using Archimedes principle with xylene as immersing liquid. The relation used is

$$D\left(gm/cm^3\right) = \frac{W_a}{W_a - W_b} D_X \qquad (10)$$

where W_a is the weight of glass sample in air, W_b is the weight of glass sample when immersed in xylene and D_x is the density of xylene (0.86 gm/cm^3). The refractive index (n) of the prepared samples was measured by the Brewster angle method using He-Ne laser (633 nm). The optical absorption spectra of all the polished samples were recorded on a Varian-Carry 5000 spectrophotometer in the range 300-3200 nm. The emission spectra were recorded using Cary Eclipse fluorescence spectrophotometer with Xe arc lamp as the excitation source at wavelength of 405nm.

RESULTS AND DISCUSSION

4.1 Physical properties

From the measured values of density (D), molar volume (V_M) and refractive index (n), various other physical parameters such as Ho^{3+} ion concentration (N), dielectric constant (ε), reflection loss (R_L) of these glasses are evaluated using the conventional formulae and are presented in Table 1. Accordingly, density responds to variations in glass composition sensitively in technological practice. Density of glass, in general, is explained in terms of a competition between the masses and size of the various structural groups present in glass. The values of D as well as V_M and various other parameters are found to increase with increasing Bi_2O_3 content in the glass systems. This is an expected result as the heavy metal oxide (Bi_2O_3) replaces the lighter oxides (B_2O_3).

4.2 Absorption spectra analysis:

The absorption spectra of 0.5 mol% of Ho^{3+} doped zinc bismuth borate glasses in UV–VIS and NIR regions are shown in Fig. 1. The assignments of the absorption bands originating from the ground level $^5I_8$ to various excited levels within the 4f shell are also shown in Fig. 1. The absorption spectra contains various bands and are assigned to the transitions $^5I_8 \rightarrow {}^5G_5$ (416nm), $^5G_6$ (450nm), $^5F_3$ (484nm), $^5F_4$ (538nm), $^5F_5$ (642nm). The identification and assignment of energy levels are made as per the procedure outlined by Carnall et al.[15]. The experimental oscillator strengths (f_{exp}) of the absorption transitions originating from the ground level of a rare earth ions have been evaluated by measuring the integrated areas under the absorption bands from the absorption spectrum. The J–O theory has been applied to the experimentally evaluated oscillator strengths to find the J–O intensity parameters Ω_λ (λ = 2, 4 and 6) by the least square fit analysis.

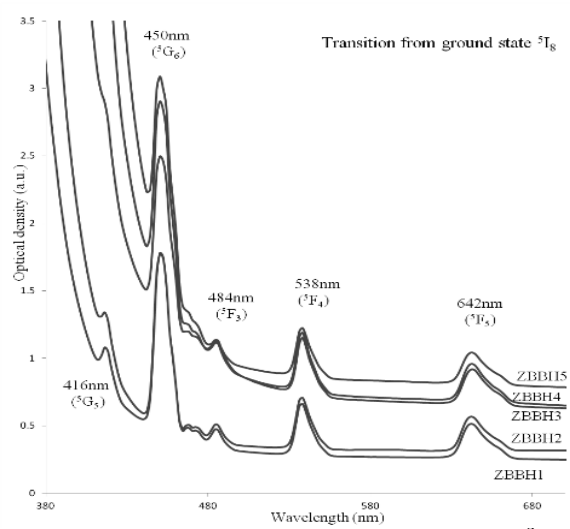

Figure 1. Optical absorption spectra of Ho^{3+} ions in $20ZnO.xBi_2O_3.(79.5-x)B_2O_3.0.5Ho_2O_3$ glass

Table 1 Density (D), molar volume (V_M), no. density of Ho^{3+} ions (N), refractive index (n), dielectric constant (ε), reflection loss (R_L) for $20ZnO.xBi_2O_3.(79.5-x)B_2O_3.0.5Ho_2O_3$ glasses.

Sample code	$x(mol\%)$	$D(g/cm^3)$	$V_M(cm^3/mol)$	$N(10^{20} ions/cm^3)$	n	$\varepsilon(n^2)$	$R_L(\%)[(n-1)/(n+1)]^2$
ZBBH1	15	4.31	30.86	2.93	1.64	2.69	5.87
ZBBH2	20	4.68	32.63	2.77	1.70	2.89	6.72
ZBBH3	25	4.85	35.55	2.54	1.72	2.96	7.01
ZBBH4	30	5.35	35.95	2.51	1.76	3.09	7.58
ZBBH5	35	5.46	38.88	2.32	1.80	3.24	8.16

The J–O parameters thus evaluated are used to calculate oscillator strength (f_{cal}) and such calculated oscillator strengths are given in Table 2 along with experimental oscillator strengths. From the absorption data, it is seen that, transition $^5I_8 \rightarrow {}^5G_5$ (416nm) gives a sharp peak for 15≤x≤20, mol % and then disappeared for x ≥ 25, mol %, it may be due to high polarizability of bismuth. The similar pattern has been seen in Ho^{3+} doped lead zinc borate glasses [18].Among the various absorption transitions of the Ho^{3+} ion, the $^5I_8 \rightarrow {}^5G_6$ (450 nm) is known as hypersensitive transition [19]. They are very sensitive to the host environment of the rare earth ion and these transitions obey the selection rules $|\Delta S| = 0$, $|\Delta L| \leq 2$, $|\Delta J| \leq 2$. The Judd- Ofelt parameters of Ho^{3+} doped zinc bismuth borate glasses have been calculated and compared with other Ho^{3+} doped hosts and are summarized in Table 3. From Table 3 it is observed that the intensity parameters Ω_λ (λ = 2, 4 and 6) for the present system follow the trend $\Omega_2 > \Omega_4 > \Omega_6$ which is similar to the behaviour observed in ZnAlBiB [20], lead- zinc- borate[18] glasses, Nd^{3+} doped zinc bismuth borate glasses.[21]

Table 2 Oscillator strength for some transitions from the indicated levels to the ground level $^5I_8$, and their root mean square (∂_{RMS}), which indicates the fit quality of theoretical and experimental results for $20ZnO.xBi_2O_3.(79.5-x)B_2O_3.0.5Ho_2O_3$ glasses.

Transitions from ground level $\rightarrow {}^5I_8$	λ (nm)	Oscillator strength (f × 10^{-7})									
		ZBBH1		ZBBH2		ZBBH3		ZBBH4		ZBBH5	
		f_{meas}	f_{cal}	f_{meas}	f_{cal}	f_{meas}	f_{cal}	f_{meas}	f_{cal}	f_{meas}	f_{cal}
$^5G_5$	416	9.93	9.94	8.03	8.88	-	-	-	-	-	-
$^5G_6$	450	27.74	27.84	35.82	35.84	62.45	62.46	76.49	76.50	107.79	107.79
$^5F_3$	484	3.45	3.52	6.23	6.43	18.23	18.67	18.05	18.95	21.43	27.57
$^5F_4$	538	7.79	7.98	9.43	10.8	32.44	32.50	19.95	23.0	30.88	34.7
$^5F_5$	642	7.65	8.10	10.24	10.55	19.39	19.60	13.91	14.8	27.91	29.3
$\partial_{RMS}(10^{-7})$		0.77		1.71		0.67		4.81		5.00	

Table 3 Judd–Ofelt intensity parameters (Ω_2, Ω_4, Ω_6) of Ho^{3+} ions doped glasses.

Glass	$\Omega_2(\times 10^{-20}\,cm^2)$	$\Omega_4(\times 10^{-20}\,cm^2)$	$\Omega_6(\times 10^{-20}\,cm^2)$	Ω_4/Ω_6
ZBBH1	2.09	1.91	1.54	1.24
ZBBH2	3.37	1.43	1.07	1.33
ZBBH3	3.43	1.32	1.21	1.09
ZBBH4	4.30	1.22	1.13	1.07
ZBBH5	4.32	1.16	1.09	1.06
ZnAlBiB glass	5.58	2.59	0.40	6.47
Lead-zinc borate glass	5.26	4.13	2.48	1.66
ZBBN1 glass	3.15	1.57	1.53	1.03

It is the fact that magnitude of Judd- Ofelt intensity parameter is related to the physical and chemical properties such as viscosity and covalent nature of the chemical bonds. In glasses, the rare earth ions are randomly distributed over nonequivalent sites with a large distribution in the crystal fields. From Table 3 it is observed that Ω_2 parameter is high. The Ω_2 parameter depends generally on the asymmetry of the sites in the neighborhood of rare earth ion. The higher the Ω_2 parameter the higher is the degree of asymmetry around the rare earth ion and stronger the covalency of rare earth ion-oxygen bond. The intensity parameters Ω_4 and Ω_6 are associated to the bulk properties such as viscosity and dielectric of the media and are also affected by the vibronic transitions of the rare earth ions bound to the ligand atoms[22] and are not as much sensitive to the medium in which the ions are located.

4.3 Fluorescence spectra analysis:

Fig. 2 shows the fluorescence spectra of Ho^{3+} doped zinc bismuth borate glasses recorded at room temperature in the wavelength region 400-800 nm, under the excitation wavelength, λ_{ext} =405nm. From the emission spectra four transitions, i.e. $^5F_3 \rightarrow {}^5I_8$, $^5F_4 \rightarrow {}^5I_8$, $^5S_2 \rightarrow {}^5I_8$, $^5F_5 \rightarrow {}^5I_8$ are observed nearly at 436, 501, 561 and 698 nm, respectively. The assignment of the peaks to specific transitions has been made on the basis of known energy levels of Ho^{3+} ions as reported by Dieke [23]. The fluorescence peak due to the transition $^5F_4 \rightarrow {}^5I_8$ appears to be intense than others. From

Table.4 The peak wavelength (λ), radiative transition probability (A_{rad}), branching ratio (β_r), stimulated emission cross-section (σ), total radiative transition probability (A_T) and the radiative life time (τ_r) and total emission cross-section (σ_t) for $20ZnO.xBi_2O_3.(79.5-x)B_2O_3.0.5Ho_2O_3$ glasses.

Transitions	λ (nm)	ZBBH1			ZBBH2			ZBBH3			ZBBH4			ZBBH5		
		A_{rad} (s^{-1})	β_r (%)	σ (10^{-22} cm^2)	A_{rad} (s^{-1})	β_r (%)	σ (10^{-22} cm^2)	A_{rad} (s^{-1})	β_r (%)	σ (10^{-22} cm^2)	A_{rad} (s^{-1})	β_r (%)	σ (10^{-22} cm^2)	A_{rad} (s^{-1})	β_r (%)	σ (10^{-22} cm^2)
$^5F_3 \rightarrow {}^5I_8$	436	304.23	0.252	2.80	316.61	0.247	2.86	372.44	0.26	3.45	376.15	0.26	3.79	392.11	0.25	3.80
$^5F_4 \rightarrow {}^5I_8$	501	616.11	0.483	6.08	621.92	0.485	6.17	684.41	0.47	6.21	692.81	0.48	6.41	770.76	0.49	6.61
$^5S_2 \rightarrow {}^5I_8$	561	74.56	0.071	2.06	89.73	0.070	2.14	105.55	0.07	2.42	106.61	0.07	2.84	111.13	0.26	3.67
$^5F_5 \rightarrow {}^5I_8$	698	211.63	0.194	4.29	253.17	0.197	4.49	270.54	0.18	4.65	270.96	0.19	4.75	313.89	0.06	4.90
A_T (s^{-1})		1206.53			1281.43			1432.94			1446.53			1587.89		
τ_r (µs)		828.82			780.37			697.86			691.31			629.76		
σ_t (10^{-22} cm^2)		15.23			15.66			16.73			17.79			18.98		

the fluorescence spectrum various parameters such as radiative transition probability ($A_{rad.}$), branching ratio (β_r), stimulated emission cross-section (σ) and the radiative life time of excited state (τ_r), etc. are calculated and these parameters are presented in Table 4.

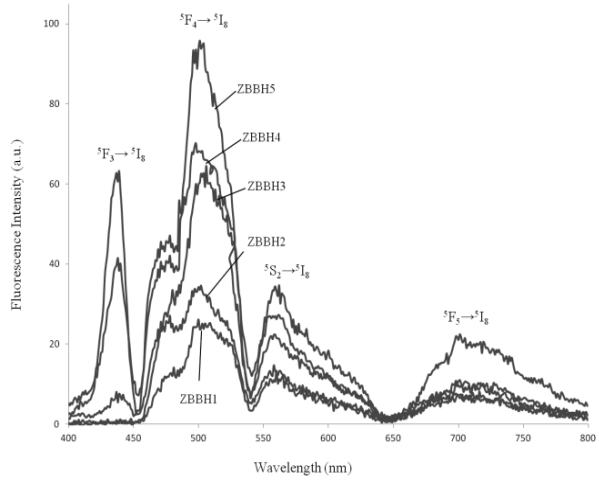

Figure 2. Emission spectra of Ho^{3+} ions in $20ZnO.xBi_2O_3.(79.5-x)B_2O_3.0.5Ho_2O_3$ glass (λ_{exc} = 405nm).

It shows that the radiative transition probability increases with increase in Bi_2O_3 content in the host glass. The trend observed in the present study follows the same pattern as reported by Sanghi et al. [24] in Er^{3+} ion doped zinc bismuth borate glass. For laser applications, the values of the emission cross-section are of great interest. A large stimulated emission cross -section is benefit for a low threshold and a high gain in laser operation. For calculating the stimulated emission cross-section, first the effective band width $\Delta\lambda$ has been calculated using the formula[25]:

$$\Delta\lambda = \frac{\int I(\lambda)d\lambda}{I(\lambda_0)}$$

where $\int I(\lambda)d\lambda$ represents the effective area of the peak and I (λ_0) is the intensity of the peak at λ_0. The stimulated emission cross-section has been calculated using Eq. (9) and are listed in Table 4.

It is observed that σ increases with increase in Bi_2O_3 content. Therefore, the large stimulated emission cross-section in the present glass is an attractive feature for low-

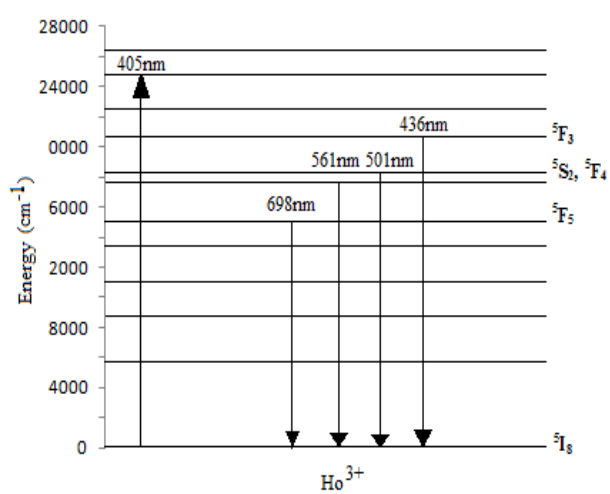

Figure 3. Lasing transitions of Ho^{3+} ions in zinc bismuth borate glasses.

threshold, high gain applications and can be utilized to obtain continuous wave (CW) laser action. The branching ratios are also evaluated for each transition. Fig.3 describes the emission transitions in terms of energy level diagram.

CONCLUSIONS

From the present study it is concluded that with the increase in bismuth content in the glass composition the density, molar volume and refractive index of the medium increases. The optical properties of Ho^{3+} ions doped zinc bismuth borate glasses have been studied. With the help of Judd–Ofelt theory, effect of bismuth oxide on the absorption and emission spectra were investigated. The variation of Judd–Ofelt intensity parameters are discussed and correlated to the structural changes in the glass network. Out of three Judd–Ofelt parameters (Ω_λ), the Ω_2 parameter shows the covalent nature of the prepared glass and I t increases with the increase in Bi_2O_3 content in the host glass The radiative properties like radiative transition probability, radiative life time, branching ratio and stimulated emission cross-section in the present glasses have been determined. The large stimulated emission cross-section in the present glass is an attractive feature for low-threshold, high gain applications and can be utilized to obtain continuous wave (CW) laser action. Based on the physical and spectroscopic properties of these glasses it could be suggested that the Ho^{3+} doped zinc bismuth borate glasses is a suitable candidate for red, near infrared and mid infrared laser and also for optical amplification.

ACKNOWLEDGEMENT

Authors are thankful to UGC, New Delhi, for providing financial support.

REFERENCES

1. E. Sintzer. Optical Maser Action of Nd^{3+} in a Barium Crown Glass. *Phys.Rev. Lett.* **1961**, 7, 444-447.
2. G. Lakshminarayana, J. Qiu, M. G. Brik, I. V. Kityk. Photoluminescent of Eu^{3+}, Tb^{3+}, Dy^{3+} and Tm^{3+} doped transparent GeO_2-TiO_2-K_2O glass ceramics. *J. Phys. Condens. Matter.* **2008**, 20, 335106 (11pp).
3. P. Nachimuthu, R. Jagannathan. Judd-Ofelt parameters, hypersensitivity, and emission characteristics of Ln(3+) (Nd^{3+}, Ho^{3+}, and Er^{3+}) ions doped in PbO-PbF_2 glasses. *J Am. Ceram. Soc.* **1999**, 82, 387-392.
4. B. Klimesz, G. Dominiak-Dzik, P. Solarz, M. Żelechower, W. Ryba-Romanowski. Optical study of GeO_2–PbO–PbF_2 oxyfluoride glass singly doped with Pr^{3+}, Nd^{3+}, Sm^{3+} and Eu^{3+}. *J. Alloys. Compd.* **2005**, 403, 76-85.
5. Y. Nageno, H. Takebe, K. Morinaga. Correlation Between Radiative Transition-Probabilities of Nd^{3+} Glasses(And Composition In Silicate, Borate, And Phosphate). *J. Am. Ceram. Soc.* **1993**, 76, 3081-3086.
6. Zhou, S., Jiang, N., Zhu, B., Yang, H., Ye, S., Laksminarayana, G., Hao, J., & Qiu, J. Multifunctional Bismuth-Doped Nanoporous Silica Glass: From Blue-Green, Orange, Red, and White Light Sources to Ultra-Broadband Infrared Amplifiers. *Adv. Funct. Mater.* **2008**, 18, 1407-1413.
7. Meng, X., Qiu, J., Peng, M., Chen, D., Zhao, Q., Jiang, X., & Zhu, C. Near Infrared Broadband Emission of Bismuth-Doped Aluminophosphate Glass. *Optics Exp.* **2005**, 13, 1628–1634.
8. Wang, Y., Dai, S., Chen, F., Xu, T., & Nie, Q. Physical Properties and Optical Band Gap of New Tellurite Glasses within the TeO_2–Nb_2O_5–Bi_2O_3 System. *Mater. Chem. Phys.***2009**, 113, 407-411.
9. Lee, S., Hwang, S., Cha, M., Shin, H., & Kim, H. Role of Copper Ion in Preventing Silver Nanoparticles Forming in Bi_2O_3–B_2O_3–ZnO Glass. *J. Phys. Chem. Solids.* **2008**, 69, 1498-1500.
10. D. Saritha, Y. Markandeya, M. Salagram, M. Vithal, A.K. Singh, G. Bhikshamaiah. Effect of Bi_2O_3 on Physical, Optical and Structural Studies of ZnO–Bi_2O_3–B_2O_3 Glasses. *J. Non-Cryst. Solids.* **2008**, 354, 5573-5579.
11. C.K. Jorgensen, Absorption Spectra and Chemical Bonding in Complexes, *Pergamon Press, Oxford,* **1962**.
12. R.D. Peacock, The Intensities of lanthanide f–f transitions in: structure and bonding, 22, Springer, Berlin, **1975**.
13. B.R. Judd, Bibliography on the Analyses of Optical Atomic Spectra: 1H-23 V, *Proc. Phys. Soc. London A* **1956**, 69 , 157.
14. M.J. Weber, D.C. Ziegler, C.A. Angell. Tailoring stimulated emission cross sections of Nd3+ laser glass: observation of large cross sections for Bids glasses. *J. Appl. Phys.* **1982**, 53, 4344.
15. W.T. Carnall, P.R. Fields, K. Rajnak. Electronic Energy Levels of the Trivalent Lanthanide Aquo Ions .II. Gd^{3+}. *J. Chem. Phys.* **1968**,49, 4443.
16. C.W. Neilson, G. Fokoster. Spectroscopic Coefficients for the p, d and f configurations. *MIT Press, Combridge, MA.* **1964**.
17. D.C. Brown. High Peak Power Nd: Glass Laser Systems. Springer, Berlin, **1981**.
18. N. Sooraj Hussain, S. Buddhudu. Absorption and emission properties of Ho^{3+} doped lead–zinc–borate glasses. *Thin Solid Films.* **2006**, 515, 318-325.
19. C.K. Jorgensen, B.R. Judd. Hypersensitive pseudoquadrupole transitions in lanthanides. *Mol.Phys.***1964**, 8, 281- 290.
20. S.K. Mahamuda, G. Vijaya Prakash. Visible Red, NIR and Mid-IR emission studies of Ho^{3+} doped Zinc Alumino Bismuth Borate Glasses. *Optical Materials.* **2013**, 36, 362-371.
21. I Pal, A Agarwal, S Sanghi. Spectroscopic and radiative properties of ND^{3+} ions doped zinc bismuth borate glases. *Indian Journal of Pure & Applied Physics.* **2013**, 51, 18- 25.
22. W.F. Krupkee. Optical absorption and fluorescence intensities in several rare earth-doped Y_2O_3 and LaF_3 sinle crystals. *Phys. Rev.* **1966**, 145, 325–337.
23. G.H. Dieke. Spectra and Energy Levels of Rare Earth Ions in Crystal. *Interscience, New York.* 1968.
24. I. Pal, S. Sanghi, A. Agarwal. Spectroscopic and structural investigations of Er^{3+} doped zinc bismuth borate glasses. *Materials Chemistry and Physics.* **2012**, 133(1) , 151-158.
25. W. Kochner. Solid-State Laser Engineering, Springer. Berlin. **1996**.
26. R. Bala, A. Agarwal, S. Sanghi, S. Khasa. Influence of SiO2 on the structural and dielectric properties of ZnO·Bi2O3·SiO2 glasses. *J. Integr. Sc. Tech.*, **2015**, 3(1), 6-13.
27. M. Roy, S. Sahu. Synthesis, electrical and thermal properties of Bi4V2-xZrxO11 (x=0.0 and 0.06) ceramics. *J. Integr. Sc. Tech.*, **2014**, 2(2), 49-51.